# Performance analysis of a solar cooling plant based on a liquid desiccant evaporative cooler

*Fabio Armanasco* [a], *Luigi Pietro Maria Colombo* [b,*], *Andrea Lucchini* [b], *Andrea Rossetti* [a]

[a] *Ricerca sul Settore Energetico s.p.a., via Rubattino 54, 20134 Milano, MI, Italy*
[b] *Dipartimento di Energia, Politecnico di Milano via Lambruschini 4, 20156 Milano, MI, Italy*

Received 22 August 2014
Received in revised form 10 January 2015
Accepted 18 January 2015 Available online 29 January 2015

## 1. Introduction

The use of air conditioning systems during summer showed considerable growth in the last few years all over the world and mainly in European residential and commercial buildings. Considerations about energy efficiency and environmental impact suggest that available heat driven cooling technologies coupled with solar thermal collectors could perform better than conventional plants based on chillers or heat pumps (Henning, 2004).

Solar cooling is a particularly interesting application of solar energy since the load is matched by the overall solar availability. In temperate climates, these systems guarantee a better utilization of solar collectors, further improving the economic performance of solar thermal systems that provide heating and domestic hot water.

* *Corresponding author*. Tel.: +39 0223993887; fax: +39 0223993913.
E-mail address: luigi.colombo@polimi.it (L.P.M. Colombo).

**Nomenclature**

*Latin symbols*

| | |
|---|---|
| A | solar collectors area, [$m^2$] |
| $a_1$ | coefficient ($a_1 = 0.974$ W $m^{-2}K^{-1}$), [W $m^{-2}K^{-1}$] |
| $a_2$ | coefficient ($a_2 = 0.005$ W $m^{-2}K^{-2}$), [W $m^{-2}K^{-2}$] |
| c | specific heat at constant pressure, [kJ $kg^{-1}$ $K^{-1}$] |
| COP | coefficient of performance (seasonal performance factor) |
| E | electric energy, [kJ] |
| F | fractional solar cooling saving |
| G | solar irradiation, [W $m^{-2}$] |
| h | humid air enthalpy referred to the unit mass of dry air, [kJ $kg_{da}^{-1}$] |
| $h_{lv}$ | liquid vapor phase transition enthalpy, [kJ $kg^{-1}$] |
| H | humid air enthalpy [kJ] |
| P | primary energy ratio |
| Q | heat exchanged, [kJ] |
| S | solar fraction |
| T | temperature, [°C] |
| t | time, [s] |
| $\dot{V}$ | volume flow rate, [$m^3$ $s^{-1}$] |
| X | absolute humidity, [kg $kg_{d.a.}^{-1}$] |
| y | generic function |
| z | generic independent quantity |

*Greek symbols*

| | |
|---|---|
| $\delta$ | percentage variation referred to the actual value |
| $\eta$ | efficiency |
| $\rho$ | dry air density, [kg $m^{-3}$] |
| $\eta_0$ | solar collector efficiency when the mean liquid temperature is equal to the outdoor temperature ($\eta_0 = 0.718$) |

*Subscripts*

| | |
|---|---|
| 0 | reference |
| a | air |
| b | backup boilers |
| c | chiller |
| d | desiccant evaporative cooler |
| da | dry air |
| e | whole plant |
| f | fuel combustion |
| g | irradiation |
| i | supply conditions |
| in | water inlet |
| l | latent |
| m | mean value between inlet and outlet |
| ma | manufacturer |
| o | outdoor conditions |
| out | water outlet |
| p | heat pump |
| q | thermal |
| r | regeneration |
| s | solar collectors |
| t | total |
| v | vapor |
| w | water |

A complete and comprehensive description of solar cooling plant configurations, including sizing criteria according to user and climate data, are available in (Henning, 2004; Wiemken, 2009). Overviews of European research on solar-assisted air conditioning are reported in (Henning, 2004; Kima and Ferreira, 2007; Henning, 2007).

Desiccant cooling systems are thermally driven open cooling cycles based on evaporative cooling and adsorption processes. The most common technology involves rotating desiccant wheels with solid material (for example zeolites), deeply investigated in terms of configurations and performance (Daou et al., 2006; Finocchiaro et al., 2012; Beccali et al., 2012; Eicker et al., 2010; Beccali et al., 2009).

On the other hand, desiccant cooling systems using a liquid solution as sorption material are a more recent development. This technology shows as major advantages:

- the possibility of high energy storage through the concentrated solution, thus allowing operation when solar energy is inadequate or even unavailable;
- low operating temperature of the liquid solution (60 ÷ 90 °C), that makes it suitable for solar energy application (Zeidan et al., 2011; Katejanekarn et al., 2009; Alizadeh, 2008; Gommed and Grossman, 2007; Crofoot and Harrison, 2012; Fong et al., 2010).

Unfortunately, the liquid desiccant technology still presents high investment cost (Henning, 2007). This drawback can be obviously overcome, if better performance and higher energy saving compared to traditional technologies are achieved.

Ricerca sul Settore Energetico S.p.A. (RSE) has been studying solar cooling technologies for some years (Viani et al., 2013; Rossetti et al., 2013a, 2013b). In particular, the work presented in this paper is included in a research activity aimed at monitoring the performance of large scale (>20 kW) solar cooling plants installed in Italy. Actually, systematic test on the performance of small scale systems (<20 kW) is already available (IEA Report). This analysis shows that for such systems the closed loop solution with single effect absorption chiller and low temperature collectors prevails on the other ones. Differently, the plant described in this work represents one of the prototypal plants with lithium chloride – water mixture desiccant evaporative cooling technology installed in Italy. The performance has been evaluated according to a shared monitoring procedure (Napolitano et al.).

## 2. Experimental plant

The Kloben facility, located near the city of Verona in Italy, is an industrial warehouse (surface 14,000 $m^2$) with an office

area (surface 1200 $m^2$). To meet the heating and cooling needs, it is endowed with an air conditioning system that can be powered by a renewable energy source like solar radiation as well as by electric energy and fossil fuels. Fig. 1 shows the main components of the air conditioning system:

- the air treatment unit that performs the dehumidification process and heat recovery; notice that the heat recovery alone is usually not enough to cool the air till the required temperature at the inlet of the warehouse;
- the reversible geothermal heat pump that provides the cold water to the fan coils in the warehouse to complete air cooling;
- the solar collectors with backup boilers.

During winter season, the plant operates in the heating mode: the dehumidification process is turned off and the desiccant evaporative cooler (DEC) operates only to ensure air exchange and heat recovery since it cannot work as a heat pump. Solar energy is directly sent to the distribution network (air and water), thus operation under winter conditions will not be considered in this paper. Fig. 2 reports a detailed scheme of the plant for summer operation. The various components are described in the following.

The authors performed a monitoring activity of the plant that was designed by a third part and is made of commercial components. Design details are proprietary. On the other hand, post processing of the readings highlighted the match between the indoor conditions and the set points, which assures the proper design of both the plant and the control system, as shown in Appendix A.

### 2.1. *Desiccant evaporative cooler (DEC)*

The air treatment unit consists mainly of two elements: a heat exchanger and a dehumidifier. The first one cools the air flow headed to the facility (supply air) by indirect evaporative cooling of hot water sprayed in the air flow coming from the facility (return air). The second one makes use of a liquid mixture of lithium chloride and water to absorb vapor from the supply air. In order to operate continuously, it is necessary to restore the original concentration of the mixture (regeneration) by discharging the water removed during the dehumidification process in a dedicated air flow (regeneration air). Hence, there are four lines in the unit, three for the air flows (the supply air line, the return air line, the regeneration air line) and one for the lithium chloride – water solution.

The nominal performance data for the air treatment unit are listed below:

- maximum air volume flow rate: 12,000 $m^3\ h^{-1}$
- maximum refrigeration power: 89 kW;
- regeneration process thermal power: 65 kW
- maximum refrigeration power related to dehumidification: 40 kW

#### 2.1.1. *Supply air line*

The desiccant evaporative cooler performs two operations to set the supply air at the facility inlet condition: an innovative process to remove moisture and a heat transfer process at constant absolute humidity consisting of indirect evaporative cooling. Referring to Fig. 2, the first operation takes place in the absorber, where a concentrated mixture of lithium chloride (Li Cl, solvent) – water ($H_2O$, solute), i.e. the strong solution, is injected in the moist air flow removing vapor by absorption. The strong solution, coming from a storage tank, before the injection, is cooled in a plate heat exchanger by the tap water employed for the indirect evaporative chilling process. The second operation takes place in a heat cross-counterflow exchanger suitably designed: the supply air flows in one side whereas in the other, hot water (warmed, as mentioned above, by the strong solution) is injected in the return air and evaporates. Finally, the supply air is sent to the user.

#### 2.1.2. *Return air line*

A fan blows the return air through the DEC unit to perform the indirect evaporative chilling process, as mentioned in Section 2.1.1, then return air and the regeneration air are mixed (exhaust air) and discharged in the atmosphere.

#### 2.1.3. *Regeneration air line*

The regeneration process requires to warm the mixture between 50 °C and 70 °C and then to spray it in the regeneration air flow. Heating is performed by the hot water from the solar collector and/or the backup boilers if solar energy is not enough. The air flow increases its humidity due to the

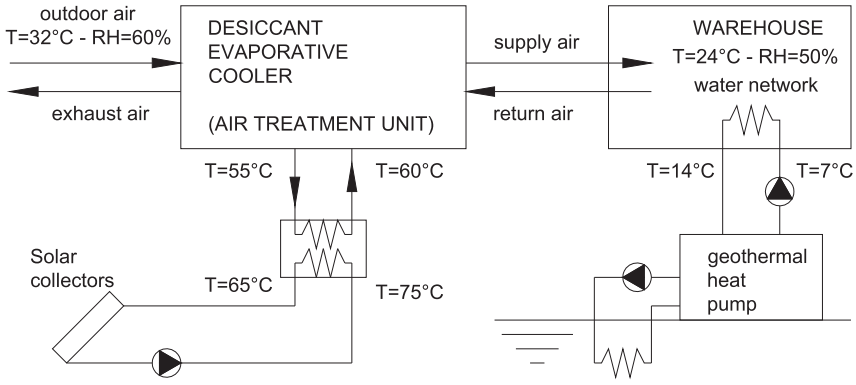


**Fig. 1 – Basic scheme of the plant.**

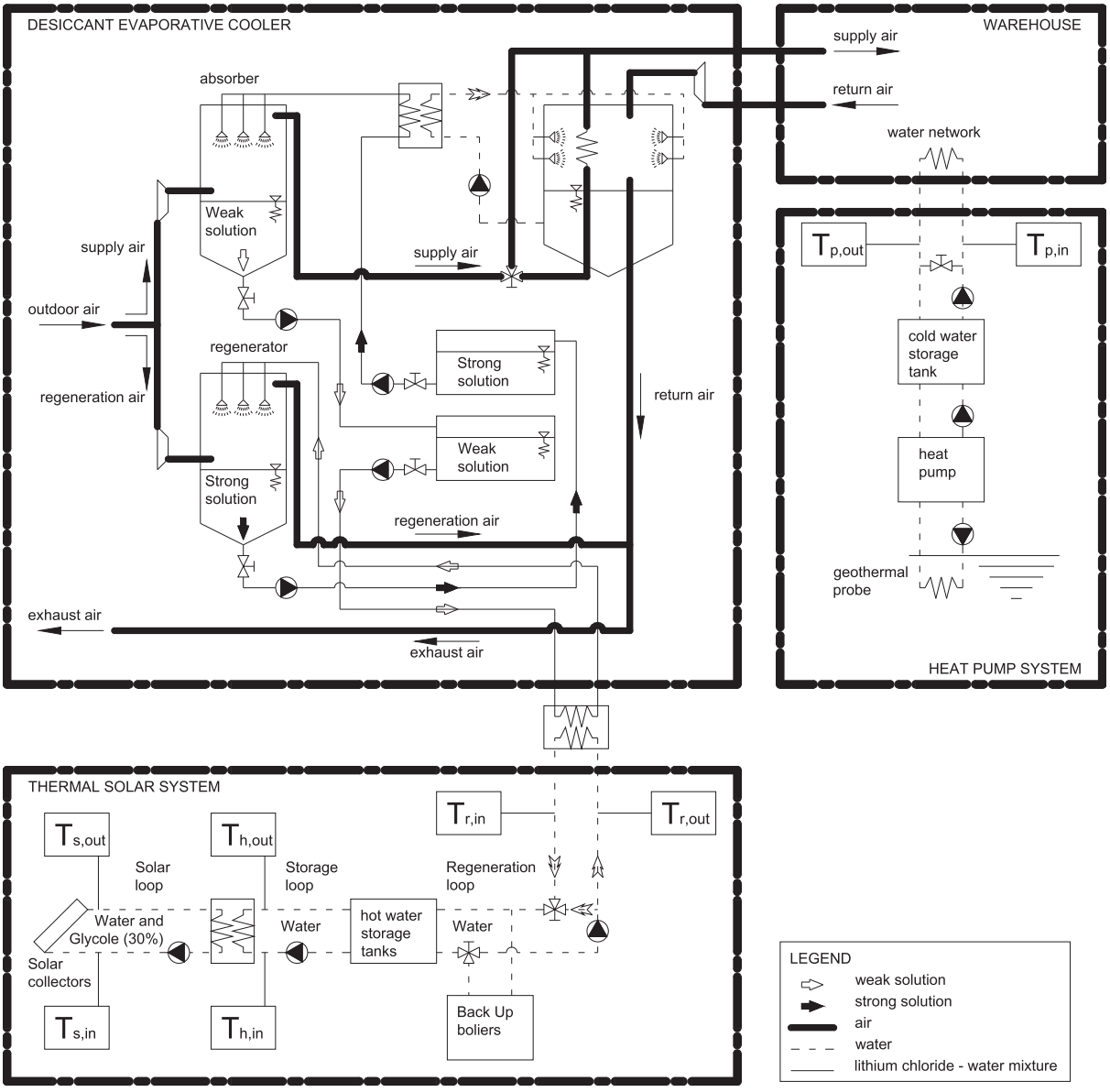


**Fig. 2 – Scheme of the plant during summer operation.**

desorption process from the sprayed weak solution. Finally, the air flow at the outlet of the regenerator is treated as exhaust air (see Section 2.1.2).

*2.1.4. Lithium chloride – water mixture circuit*

The mixture loop is made of six components: an absorber, a regenerator, two heat exchangers and two storage tanks (one for the strong solution and one for the weak solution). Storage allows continuous operation regardless the weather conditions and it is designed to maximize solar energy exploitation. During the dehumidification process, the strong solution is pumped from the tank to a heat exchanger where it is cooled by the water used for the evaporative cooling process (see Section 2.1.1). Then, it enters the absorber where it is sprayed in the supply air flow. Because of the absorption process, the supply air humidity reduces and the solution becomes weak. The weak solution is periodically pumped to its own tank. Once the latter is full, the regeneration process takes place. At first, the weak solution is drawn to a heat exchanger, fed by hot water from the solar collectors to be heated within 50 °C and 70 °C. Then it is sprayed in the regenerator supplied with the regeneration air flow. The subsequent desorption process restores the original concentration of lithium-chloride and the resulting strong solution is periodically pumped to its own tank. On average, during summer, the regeneration process occurs three times a day.

## 2.2. *Reversible geothermal heat pump*

During summer, the reversible geothermal heat pump (Tonon Forty EPH 040) is used to produce cold water (temperature range: 15 °C ÷ 18 °C), which is stored in a tank (volume: 1.5 $m^3$).

A pump provides the flow in the radiators of the water network.

The nominal performance data during summer are listed below:

- refrigeration power: 43.2 kW;
- compressor power: 13.2 kW;
- chilling efficiency: 3.3

The heat pump is connected to a ground heat rejection system (14 geothermal probes: diameter 40 mm, length 100 m) with three dedicated pumps suitably activated according to the thermal load. The circuit is filled with 30% water-glycol mixture.

### 2.3. *Thermal solar system*

The solar system is composed by three loops, briefly described in the following.

1 The solar loop, filled with 30% water-glycol mixture, has three main components: a heat exchanger, a circulation pump and 72 Kloben solar collectors, concentrated vacuum tube type model SKY 12 CPC 58, partially covering the facility roof, with 136.1 $m^2$ tapping surface and 155.5 $m^2$ gross surface. The heat exchanger provides the hot water to heat the weak solution in order to start the regeneration process.
2 The storage loop connects the heat exchanger of the solar loop with two tanks that store the hot water needed for the regeneration process. Hence, the plant can operate regardless the weather conditions. The tanks have a total buffer volume of 8 $m^3$ and are thermally insulated. A control logic allows regulating the temperature of each tank separately.
3 The regeneration loop provides the hot water to the heat exchanger used to warm the weak solution. If the solar collectors cannot provide the required energy, a by-pass redirects the water flow to four backup boilers (inlet temperature 60 °C, outlet temperature 80 °C, thermal power 23.6 kW, natural gas volume flow rate 2.57 $stm^3/h$).

### 2.4. *Operating conditions*

In summer, the air conditioning system operates only during the day, approximately for twelve hours, from 7 a.m. to 7 p.m. It regulates the temperature (which may change from area to area of the building, the minimum set point is 20 °C) and the relative humidity (the set point lies in the range 50% ÷ 60%) in the facility. Both the DEC unit and the geothermal heat pump, each regulated by a local control system, contribute to set the temperature. The former provides the supply air to the building while the latter feeds the radiators with cold water (the inlet temperature is in the range 12 °C ÷ 16 °C). On the other hand, only the DEC unit regulates the humidity: the set point for the supply air is 9 $g/kg_{da}$, thus the activation of the absorber takes place when the humidity ratio of the return air overcomes this value.

The control strategy of the solar field is defined in order to maximize primary energy saving. The pumps of the regeneration loop only work when regeneration is needed, while the pumps of the solar and storage loops are switched on together if the water temperature at the outlet of the solar field is 10 °C higher than the temperature at the top of the storage tanks.

## 3. Measurement devices

A data acquisition system records the output of every instrument with a frequency of 0.1 Hz (period 10 s) and calculates the mean value over ninety samples. The list of the measured quantities is reported in Table 1 together with the experimental uncertainty.

As the pumps operate at constant speed, volume flow rates have been preliminary measured by an ultrasonic meter with 3% uncertainty and considered constant over the whole observation period.

## 4. Methodology of analysis

Weather conditions strongly affect the operating point of the plant. The energy consumption for dehumidification and cooling depends on the difference of the temperature and the moisture content of the outdoor air from their respective set points, while the energy saving is related to the amount of solar energy that can be used for the regeneration process of the liquid desiccant mixture. Consequently, a proper methodology of analysis (Napolitano et al.,) has been followed to evaluate the plant performances. As mentioned above, there are three main quantities affecting the system behavior: the outdoor temperature (T), the outdoor absolute humidity (X) and the energy provided by solar irradiation (G). Since all of them are time dependent and vary in wide ranges (their variation intervals are: $T \in [14; 41]$ °C; $X \in [6; 22]$ $g/kg_{da}$; $G \in [0; 1.1]$ kW $m^{-2}$), a statistical analysis of the readings, reported in Appendix B, was performed to ascertain whether it were possible to define a typical day, in order to analyze the operating conditions of the plant on a daily base. However, the distributions of the outdoor temperature (T), the outdoor absolute humidity (X) and the solar irradiation (G) turned out to have large standard deviations (to gather the 50% of the data it is necessary a portion of the range that is between one fourth and one third of the span). In conclusion:

- it is not possible to define a "standard" day and analyze the operating condition on a daily base;
- the daily variability is too high, so that performances has been evaluated monthly and on the whole monitoring period;
- the variability of the weather conditions makes the daily values of the energy quantities not very meaningful.

The components of the air conditioning system, that are designed to work at constant operating conditions, do not run continuously. As an on/off control logic is adopted, reference is made to energy instead of power to properly evaluate the plant performance. The guidelines reported by IEA in

**Table 1 – Installed instrumentation, measured quantities and relative uncertainty.**

| Quantity | Measuring device | Range | Uncertainty |
|---|---|---|---|
| **Solar loop** | | | |
| Solar radiation | LSI-LASTEM C101R first class thermopile global radiometer | 0 ÷ 1500 W $m^{-2}$ | 2.5% |
| Solar panel inlet temperature | NTC10K | 0 ÷ 200 °C | ±0.1 °C |
| Secondary loop heat exchanger inlet temperature | NTC10K | 0 ÷ 200 °C | ±0.1 °C |
| Secondary loop heat exchanger outlet temperature | NTC10K | 0 ÷ 200 °C | ±0.1 °C |
| Solar panel outlet temperature 1 | PT100 | 0 ÷ 200 °C | ±0.1 °C |
| Solar panel outlet temperature 2 | PT100 | 0 ÷ 200 °C | ±0.1 °C |
| Solar panel outlet temperature 3 | PT100 | 0 ÷ 200 °C | ±0.1 °C |
| 1° hot water storage tank temperature 1/2/3/4 | NTC 10K | 0 ÷ 200 °C | ±0.1 °C |
| 2° hot water storage tank temperature 1/2/3/4 | NTC 10K | 0 ÷ 200 °C | ±0.1 °C |
| Regeneration loop heat exchanger inlet temperature | NTC10K | 0 ÷ 200 °C | ±0.1 °C |
| Regeneration loop heat exchanger outlet temperature | NTC10K | 0 ÷ 200 °C | ±0.1 °C |
| **Desiccant evaporative cooler (DEC)** | | | |
| Outdoor air temperature | PT100 LASTIM DMA875 | −30 ÷ +70 °C | ±0.1 °C |
| Outdoor air relative humidity | Hygrometer LASTIM DMA875 | 0 ÷ 100 RH | 1.5% |
| Supply air temperature | PT100 by DEC Manufacturer | −30 ÷ +70 °C | ±0.1 °C |
| Supply air relative humidity | Hygrometer by DEC Manufacturer | 0 ÷ 100 RH | 1.5% |
| Supply air volume flow rate | Inverter by DEC manufacturer | 40 ÷ 100% | 1% |
| Return air temperature | PT100 by DEC Manufacturer | −30 ÷ +70 °C | ±0.1 °C |
| Return air relative humidity | Hygrometer by DEC Manufacturer | 0 ÷ 100 RH | 1.5% |
| Return air volume flow rate | Inverter by DEC manufacturer | 40 ÷ 100% | 1% |
| Regeneration outdoor air flow rate | Inverter by DEC manufacturer | 40 ÷ 100% | 1% |
| Electrical absorbed power | Electric net analyzer Siemens 7KT1 340 | 0 ÷ 50 kW | 0.8% |
| **Geothermal heat pump** | | | |
| Cold water storage tank inlet temperature | NTC10K | −30 ÷ +70 °C | ±0.1 °C |
| Cold water storage tank outlet temperature | NTC10K | −30 ÷ +70 °C | ±0.1 °C |
| Geothermal heat exchanger inlet temperature | NTC10K | −30 ÷ +70 °C | ±0.1 °C |
| Geothermal heat exchanger outlet temperature | NTC10K | −30 ÷ +70 °C | ±0.1 °C |
| | Electric net analyzer Siemens 7KT1 340 | 0 ÷ 50 kW | 0.8% |
| **Whole plant** | | | |
| Electrical absorbed power | Electric net analyzer Siemens 7KT1 340 | 0 ÷ 50 kW | 0.8% |

(Napolitano et al.,), specifically developed for solar heating and cooling systems, have been adopted to evaluate performance indices. Accordingly, the useful effect is the sum of four terms: heat for space heating; heat for domestic hot water; heat removed by the cooling elements; enthalpy difference of the air between outdoor and supply condition. The above quantities are determined from the measured data as explained hereafter.

The humid air enthalpy referred to the unit mass of dry air (air specific enthalpy) is:

$$h = c_a T + X(h_{lv} + c_v T) \tag{1}$$

Hence, the useful effect is the air enthalpy variation from inlet to outlet, calculated as:

$$\Delta H = \int_{t_0}^{t_1} \rho_a \dot{V}_a (h_o - h_i) dt \tag{2}$$

Similarly, the heat exchanged by any water flow in any loop of the plant is expressed in terms of enthalpy variation from inlet to outlet:

$$Q = \int_{t_0}^{t_1} \rho_w \dot{V}_w c_w |T_{out} - T_{in}| dt \tag{3}$$

Energy inputs are:

1. electric energy consumption of the whole plant ($E_e$), directly read from the net analyzer;
2. energy required for the regeneration of the mixture: $Q_r$, according to Equation (3).

The latter is provided by a hot water flow, warmed by solar collectors or conventional boilers. Solar radiation provides the energy

$$Q_g = \int_{t_0}^{t_1} AG dt \tag{4}$$

The fraction of $Q_g$ transferred to the water in the solar loop, named $Q_s$, is evaluated by Equation (3). If it is lower than required by the regeneration process, the backup boilers provide the difference:

$$Q_b = \begin{cases} Q_r - Q_s & if \quad Q_r > Q_s \\ 0 & if \quad Q_r \le Q_s \end{cases} \tag{5}$$

The IEA report (Napolitano et al.,) groups performance indices in three categories: overall system performance, solar energy exploitation, primary energy usage and saving of a plant endowed with a solar energy cooling system. In the first category, three coefficients of performances are defined:

1. thermal coefficient of performance (ratio of the useful effect to the heat required for the mixture regeneration):

$$COP_q = \frac{\Delta H}{Q_r} \tag{6}$$

2. electric coefficient of performance (ratio of the useful effect to the electric energy supplied to the DEC):

$$COP_e = \frac{\Delta H}{E_d} \tag{7}$$

3. overall coefficient of performance (ratio of the useful effect to the total energy input):

$$COP_t = \frac{\Delta H}{Q_r + E_d} \tag{8}$$

Solar energy exploitation is quantified by the ratio of the energy provided by the sun ($Q_s$) to the heat required for the mixture regeneration, including the possible contribution of backup boilers ($Q_b$):

$$S = \frac{Q_s}{Q_r} = \frac{Q_s}{Q_s + Q_b} \tag{9}$$

The conversion efficiency of the solar field is defined as:

$$\eta = \frac{Q_s}{Q_g} \tag{10}$$

The manufacturer of the solar collectors provides specific coefficients ($\eta_0$, $a_1$, $a_2$) for an empirical correlation to evaluate the conversion efficiency of a single collector, which was used for comparison:

$$\eta_{ma} = \eta_0 - a_1\frac{T_m - T_o}{G} - a_2\frac{(T_m - T_o)^2}{G} \quad \begin{cases} \eta_0 = 0.718 \\ a_1 = 0.974 \ W/m^2K \\ a_2 = 0.005 \ W/m^2K^2 \end{cases} \tag{11}$$

Primary energy usage is quantified by the primary energy ratio ($P_d$), i.e. the ratio of the useful effect to the primary energy necessary to fulfill the requirements of the system.

Hence, for the desiccant evaporative cooler it is expressed as:

$$P_d = \frac{\Delta H}{\frac{Q_b}{\eta_b \eta_f} + \frac{E_d}{\eta_e}} \tag{12}$$

where $\eta_e$ is a typical value of the conversion efficiency for a state of the art power plant ((Napolitano et al.) suggests $\eta_e = 0.40$); $\eta_b$ is a typical value of the conversion efficiency for a state of the art boiler ((Napolitano et al.) suggests a combustion efficiency $\eta_f = 0.90$, whereas for the backup boilers the nominal value is $\eta_b = 0.95$).

For the whole plant the primary energy ratio ($P_e$) is analogously defined as:

$$P_e = \frac{\Delta H + Q_c}{\frac{Q_b}{\eta_b \eta_f} + \frac{E_e}{\eta_e}} \tag{13}$$

where the useful effect includes the heat removed by the radiators fed by cold water from the geothermal heat pump ($Q_c$) and the electric energy consumption includes the contribution of the circulation pumps in both the chiller and the solar field. $\eta_b$, $\eta_e$ and $\eta_f$ are the same as in Equation (12).

Primary energy saving is quantified by the primary energy saving index (F). Given a standard (state of the art) technology and an alternative technology, the difference in the primary energy consumption is compared to the primary energy consumption of the standard technology. It follows:

$$F = 1 - \frac{\frac{Q_b}{\eta_b \eta_f} + \frac{E_e}{\eta_e}}{\frac{Q_{b,0}}{\eta_b \eta_f} + \frac{Q_{c,0}}{COP_0 \eta_e} + \frac{E_0}{\eta_e}} \tag{14}$$

where the subscript 0 refers to the standard technology. The IEA report (Napolitano et al.,) suggests $COP_0 = 2.8$ for conventional compression chillers.

Analysis of uncertainty based on the overall experimental data set, according to UNI CEN 13005, has been performed for all the computed variables and global indices of performance. Table 2 reports the result for the latter.

## 5. Results

### 5.1. *Solar system*

The average conversion efficiency of the solar field (Equation (10)), has been calculated on a monthly base. The results, reported in Table 3, show that the empirical correlation provided be the manufacturer for a single collector (Equation (11)) largely overestimates the conversion efficiency of the solar field, consequently it cannot be used as a design tool. As no information is available about the procedure followed by the manufacturer to evaluate the single collector efficiency, it is not possible to understand the origin of such disagreement. Nevertheless, the solar system shows high performances: the percentage primary energy saving is always greater than 90% and the average coefficient of performance referred to the electric consumption is 25.8. Furthermore, during the observation period, the energy demand of the regeneration process has been always lower than the energy stored in the hot water tank by the solar collector. Hence, backup boilers have never been turned on and primary energy consumption has been only due to the pumps.

**Table 2 – Uncertainty for the global indices of performance.**

| Quantity | Uncertainty [%] |
|---|---|
| Refrigeration energy | 6.7 |
| Latent load | 8.4 |
| Sensible load | 7 |
| Regeneration load | 7.5 |
| Electrical load | 0.8 |
| Absorber efficiency | 11 |
| Thermal COP | 10 |
| Electrical COP | 6.7 |
| Global COP | 9.3 |
| Primary energy saving index F | 5 |
| Primary energy ratio P | 8.4 |

**Table 3 – Efficiency of the solar collectors field and performance evaluation of the solar system.**

| Month | | | July | August | September | Seasonal (average) |
|---|---|---|---|---|---|---|
| Period | | | 12 ÷ 31 | 1 ÷ 31 | 1 ÷ 19 | |
| Duration | | day | 20 | 31 | 19 | 70 |
| Energy provided by solar irradiation | $Q_g$ | MWh | 18.1 | 27.8 | 12.7 | 58.6 |
| Energy provided by solar irradiation per day (average value of the period) | | MWh day$^{-1}$ | 0.91 | 0.90 | 0.67 | 0.84 |
| Energy transferred to water (measured) | $Q_s$ | MWh | 6.7 | 13.1 | 5.1 | 24.9 |
| Energy stored in the hot water tank | $Q_h$ | MWh | 6.49 | 11.30 | 4.99 | 22.76 |
| Energy provided by the back up boilers | $Q_b$ | MWh | 0 | 0 | 0 | 0 |
| Electric energy consumption | $E_s$ | kWh | 226 | 433 | 220 | 879 |
| Collectors field efficiency (calculated) | $\eta$ | – | 0.37 | 0.47 | 0.40 | 0.42 |
| Collector efficiency (manufacturer) | $\eta_{ma}$ | – | 0.64 | 0.65 | 0.64 | 0.65 |
| Primary energy ratio | P | – | 11.46 | 10.38 | 9.07 | 10.33 |
| Percentage primary energy saving | F | – | 92.54% | 91.77% | 90.58% | 91.72% |
| Coefficient of performance | $COP_e$ | – | 28.65 | 25.69 | 22.68 | 25.83 |

### 5.2. *Desiccant evaporative cooler (DEC)*

Table 4 reports a summary of the operating conditions and performance indices of the desiccant evaporative cooler.

The DEC unit allows significant values of primary energy saving (the average value on the overall monitoring period is 42.5%). However, monthly variation is considerable, which is related to both the weather and operating conditions (in particular, the volume flow rate varies significantly, depending on the settings of the control system). The seasonal primary energy ratio is 2.58, always higher than the values attained by the standard systems. The highest performance occurs in July ($P_d = 4.20$).

The electric coefficient of performance is on average 2.5 times greater than $COP_0$ (standard compression chiller) because the electric consumption is only related to pumping power. The comparison between the values of the thermal coefficient of performance and the overall coefficient of performance suggests that most of the energy input is used for the regeneration process of the lithium-chloride mixture. Thus, it is interesting to consider in more detail the absorption and desorption processes.

Data reported in Table 5 show that the absorption efficiency is lowest in July. This is mostly due to the difference between the operating conditions (in July the humidity removal is the lowest of the whole monitoring period) and the design conditions, corresponding to the worst case, i.e. humidity removal equal to 4.0 g $kg_{da}^{-1}$.

Desorber data are reported in Table 6. The regeneration process of the lithium chloride – water mixture shows similar

**Table 4 – Desiccant evaporative cooler average operating conditions and average performance coefficients.**

| Month | | | July | August | September | Seasonal (average) |
|---|---|---|---|---|---|---|
| Period | | | 12 ÷ 31 | 1 ÷ 4; 17 ÷ 28 | 1 ÷ 19 | |
| Duration | | days | 20 | 16 | 19 | 55 |
| Outdoor air temperature | $T_o$ | °C | 23.8 | 27.5 | 22.7 | 24.5 |
| Outdoor air humidity | $X_o$ | g $kg_{da}^{-1}$ | 10.8 | 12.5 | 10.7 | 11.3 |
| Air volume flow rate | $V_a$ | m$^3$ h$^{-1}$ | 5650 | 4506 | 6207 | 5509 |
| Thermal power: total | | kW | 16.1 | 18.1 | 20.2 | 18.1 |
| Thermal power: sensible | | kW | 12.7 | 13.0 | 17.7 | 14.5 |
| Thermal power: latent | | kW | 3.4 | 5.1 | 2.5 | 3.6 |
| Air enthalpy variation | $\Delta H$ | MWh | 7.364 | 6.714 | 8.233 | 22.311 |
| Air enthalpy variation per day (average value of the period) | | MWh day$^{-1}$ | 0.368 | 0.420 | 0.433 | 0.406 |
| Regeneration heat | $Q_r$ | MWh | 6.492 | 6.835 | 4.924 | 18.252 |
| Regeneration heat per day (average value of the period) | | MWh day$^{-1}$ | 0.325 | 0.427 | 0.259 | 0.332 |
| Mean regeneration water temperature | | °C | 51.1 | 52.4 | 50.6 | 51.4 |
| Electric energy ATU | | MWh | 1.764 | 1.028 | 1.792 | 4.584 |
| Electric energy ATU per day (average value of the period) | | kWh day$^{-1}$ | 88.2 | 64.3 | 94.3 | 83.3 |
| Electric energy ATU auxiliaries | | MWh | 0.473 | 0.388 | 0.266 | 1.127 |
| Electric energy DEC | $E_d$ | MWh | 1.291 | 0.640 | 1.526 | 3.457 |
| Thermal coefficient of performance | $COP_q$ | – | 1.13 | 0.98 | 1.67 | 1.22 |
| Electric coefficient of performance | $COP_e$ | – | 5.70 | 10.49 | 5.40 | 6.45 |
| Overall coefficient of performance | $COP_t$ | – | 0.95 | 0.90 | 1.28 | 1.03 |
| Primary energy ratio | $P_d$ | – | 2.28 | 4.20 | 2.16 | 2.58 |
| Primary energy ratio: reference chiller | $P_0$ | – | 1.12 | 1.12 | 1.12 | 1.12 |
| Primary energy saving | $F_d$ | – | 32.9% | 57.1% | 39.1% | 42.5% |

**Table 5 – Average operating conditions of the absorber.**

| Month | | | July | August | September | Seasonal (average) |
|---|---|---|---|---|---|---|
| Period | | | 12 ÷ 31 | 1 ÷ 4; 17 ÷ 28 | 1 ÷ 19 | |
| Duration | | days | 20 | 16 | 19 | 55 |
| Air enthalpy variation: total | $\Delta H$ | MWh | 7.36 | 6.71 | 8.23 | 22.30 |
| Air enthalpy variation: latent | $\Delta H_l$ | MWh | 1.60 | 2.05 | 1.48 | 5.13 |
| Regeneration heat | $Q_r$ | MWh | 6.49 | 6.84 | 4.92 | 18.25 |
| Absorber efficiency | $\Delta H_l/Q_r$ | | 0.25 | 0.30 | 0.30 | 0.28 |
| Outdoor air humidity | $X_o$ | $g/kg_{da}^{-1}$ | 10.8 | 12.5 | 10.7 | 11.3 |
| Supply air humidity | $X_i$ | $g/kg_{da}^{-1}$ | 8.5 | 8.9 | 7.4 | 8.3 |
| Humidity removal | | $g/kg_{da}^{-1}$ | 2.3 | 3.6 | 3.3 | 3.0 |

energy needs in July and August whereas in September the required regeneration power lowers because of the decrease in both temperature and specific humidity of the outdoor air. It is worth noting that the average inlet temperature of the water, used to warm the mixture in the regeneration process, is close to the lower limit of the operating range, i.e. 50 °C. Thus, even though the solar radiation provides all the energy required by the regeneration process ($Q_g > Q_r$ see Tables 3 and 5), a further increase (about 5 °C) of the inlet water temperature would promote the process efficiency. This could be achieved by a different design of the solar field as well as changing the control logic of backup boilers. The latter would affect in turn the primary energy saving. Hence, this opportunity should be carefully evaluated.

### 5.3. *Geothermal heat pump*

The coefficient of performance of the geothermal heat pump is around 2.9 for all the observed period with negligible variations (Table 7). This value is slightly larger than the standard (2.8). On the other hand, the electric consumption for geothermal field pumps is significant and can easily attain 10–15% of the overall electrical need.

### 5.4. *Overall plant*

Plant performances are reported in Table 8. The geothermal heat pump and the desiccant evaporative cooler share the chilling process almost alike. An air conditioning system made of a water loop cooled by a standard compression chiller with $COP_0 = 2.8$ is taken as a term of comparison: the plant seasonal primary energy ratio results about 1.5 times greater and allows about 30% primary energy saving.

## 6. Conclusions

The solar-aided plant performs always better than a conventional air conditioning system based on a compression chiller and a water loop (standard system). Hence, from a technical standpoint, the combination of the liquid desiccant evaporative cooler with the solar collectors proves to be a promising solution for solar cooling and a valuable alternative to conventional air treatment units. On the other hand, the absorber unit always operates near the lower bound of the nominal temperature range. Therefore, higher performance could be achieved by optimizing the solar system design.

**Table 6 – Average operating conditions of the desorber.**

| Month | | | July | August | September | Seasonal (average) |
|---|---|---|---|---|---|---|
| Period | | | 12 ÷ 31 | 1 ÷ 4; 17 ÷ 28 | 1 ÷ 19 | |
| Duration | | days | 20 | 16 | 19 | 55 |
| Regeneration thermal power | | kW | 55.3 | 57.0 | 51.2 | 54.4 |
| Regeneration energy | $Q_r$ | MWh | 6.492 | 6.835 | 4.924 | 18.252 |
| Inlet water temperature | $T_{r,in}$ | °C | 54.7 | 55.9 | 53.7 | 54.7 |
| Outlet water temperature | $T_{r,out}$ | °C | 47.5 | 48.9 | 47.5 | 47.9 |
| Temperature difference | | °C | 7.2 | 7.0 | 6.2 | 6.8 |
| Number of regeneration | | | 53 | 40 | 25 | 118 |
| Number of daily regenerations | | | 2.65 | 2.50 | 1.32 | 2.15 |

**Table 7 – Geothermal heat pump indices of performances.**

| Month | | | July | August | September | Seasonal (average) |
|---|---|---|---|---|---|---|
| Period | | | 12 ÷ 31 | 1 ÷ 31 | 1 ÷ 19 | |
| Duration | | days | 20 | 31 | 19 | 70 |
| Refrigeration power | | kW | 38.80 | 43.60 | 42.80 | 42.01 |
| Heat removed | $Q_p$ | MWh | 7.73 | 13.40 | 7.27 | 28.40 |
| Electric energy | $E_p$ | MWh | 2.83 | 4.38 | 2.49 | 9.70 |
| Coefficient of performance | COP | – | 2.73 | 3.06 | 2.92 | 2.93 |

**Table 8 – Overall plant performances.**

| Month | | | July | August | September | Seasonal (average) |
|---|---|---|---|---|---|---|
| Period | | | 12 ÷ 31 | 1 ÷ 4; 17 ÷ 28 | 1 ÷ 19 | |
| Duration | | days | 20 | 16 | 19 | 55 |
| Heat removed | $\Delta H + Q_p$ | MWh | 15.10 | 14.00 | 15.50 | 44.60 |
| Heat removed per day (average value of the period) | | MWh day$^{-1}$ | 0.755 | 0.875 | 0.816 | 0.811 |
| Regeneration heat | $Q_r$ | MWh | 6.49 | 6.84 | 4.92 | 18.25 |
| Regeneration heat per day (average value of the period) | | MWh day$^{-1}$ | 0.325 | 0.428 | 0.259 | 0.332 |
| Electric energy | $E_e$ | MWh | 4.24 | 3.06 | 3.92 | 11.22 |
| Electric energy per day (average value of the period) | | MWh day$^{-1}$ | 0.212 | 0.191 | 0.206 | 0.204 |
| Heat removed: DEC fraction | | – | 48.8% | 47.9% | 53.1% | 50.0% |
| Primary energy ratio: standard chiller | | – | 1.1 | 1.1 | 1.1 | 1.1 |
| Electric coefficient of performance | $COP_e$ | – | 3.56 | 4.58 | 3.95 | 3.98 |
| Coefficient of performance | COP | – | 1.41 | 1.41 | 1.75 | 1.51 |
| Primary energy ratio | P | – | 1.42 | 1.83 | 1.58 | 1.59 |
| Primary energy saving: chiller | $F_c$ | – | 21.4% | 38.9% | 29.2% | 29.6% |

It has to be noted that the European Standard EN 15603 (Energy performance of buildings – Overall energy use and definition of energy ratings) (EN 15603, 2007) prescribes the values for the standard efficiencies ($\eta_b$, $\eta_e$, $\eta_f$) and the coefficient of performance ($COP_0$), to be used for energy indices evaluation. These figures slightly differ from the ones suggested by IEA (Napolitano et al.,). Moreover, the values indicated are not the same all over the world, and the performance of standard technologies is continuously improving. Thus, a sensitivity analysis, reported in Appendix C, has been carried out to understand the influence of the standard values variation on the primary energy ratio ($P_e$) and the primary energy saving index (F). On this basis, the following remarks can be drawn.

1. As the backup boilers remained off during the whole monitoring period, the percentage variation of the pri-mary energy ratio ($\delta P_e$) depends only on the percentage variation of the electric energy efficiency ($\delta\eta_e$). Moreover, as it is verified setting $Q_b = 0$ MWh in Equation (C.3), their values are just the same ($\delta P_e = \delta\eta_e$). Assuming reasonable variations in the electric efficiency within the range [0.40, 0.45], the subsequent changes in electric efficiency and primary energy ratio ($P_e$) turn out to vary in the range [0.0%, 12.5%].
2. Similarly to the previous point, as the backup boilers remained off during the whole monitoring period and the standard technology does not require boilers ($Q_{b,0} = 0$ MWh), the percentage variation in the primary energy saving index (F) only depends on the percentage variation of the coefficient of performance of the reference technology ($\delta COP_0$). Assuming that all the auxiliary com-ponents are embedded in the reference chiller, it follows $E_0 = 0$ MWh. The relation between the percentage variation in the primary energy saving index ($\delta F$) and the percentage variation in the coefficient of performance ($\delta COP_0$) (as it can be checked by equation (C.5) setting: $Q_b = 0$ MWh, $Q_{b,0} = 0$ MWh, $E_0 = 0$ MWh) becomes:

$$\delta F = \left(1 - \frac{1}{F}\right)\delta COP_0 \qquad (15)$$

Though the IEA report (IEA Report) indicates $COP_0 = 2.8$, it is reasonable to assume a variation range [2.6, 3.0] under real operating conditions corresponding to a percentage variation within [−7.1%, 7.1%]. As the proportionality coefficient in Equation (15) is negative, an increase in the $COP_0$ causes a reduction in the primary energy saving. The corresponding percentage variation of the primary energy saving index ($\delta F$) lies in the range [−26.1%; 26%].

3. Nevertheless, the solar-aided technology retains a significant margin in primary energy saving.

## Acknowledgments

This work has been financed by the Research Fund for the Italian Electrical System under the Contract Agreement between RSE S.p.A. and the Ministry of Economic Development - General Directorate for Nuclear Energy, Renewable Energy and Energy Efficiency in compliance with the Decree of March 8th, 2006.

## Appendix A

To keep the indoor conditions (which correspond to the warehouse conditions, as it is more than ten times larger than the office area) at the set point (temperature 24 °C, relative humidity 50%) two commercial products were used:

1. A desiccant evaporative cooler, to assure air replacement and to control the absolute humidity of the supply air (to keep it at 9 g $kg_{da}^{-1}$ in the present case). This component can set the absolute humidity of the supply air (operation performed by the absorber), but not the temperature because it was designed (as it can be seen in Fig. 2) to use the return air (coming from the warehouse) to perform heat recovery and evaporative cooling. A device to chill the air and set its temperature is missing.
2. A geothermal heat pump to provide cold water to the fan coils of the water network, installed in the warehouse, to

exchange the thermal power required to keep the indoor temperature at the set point. A thermostat turns on and off the circulation pump.

As the plant was designed by a third part, design details are proprietary including the control strategy implemented in the desiccant evaporative cooler. Nevertheless, the monitoring procedure showed that the plant and the single components work properly. Figs. A.1 and A.2 report the trends of temperatures, absolute humidity referred to a three days period (from 00:00 AM of July 27th 2011 to 00:00 AM July 30th 2013, during the whole period the volume flow rate of the supply air remained constant at the value of 4500 $m^3\ h^{-1}$). It is clearly visible in Fig. A.1 that the outdoor absolute humidity is always higher than the set point (9 g $kg_{da}^{-1}$) and it varies in the range 10 g $kg_{da}^{-1}$ ÷ 18 g $kg_{da}^{-1}$. On the contrary, when the absorber is working the absolute humidity of the supply air at the entrance of the warehouse (or equivalently at the outlet of the desiccant evaporative cooler) is at the set point. The only cause of absolute humidity change in the warehouse is the human presence. However, as few people are actually present, their contribution is negligible and the absolute humidity of the return air can be considered equal to the one of the supply air.

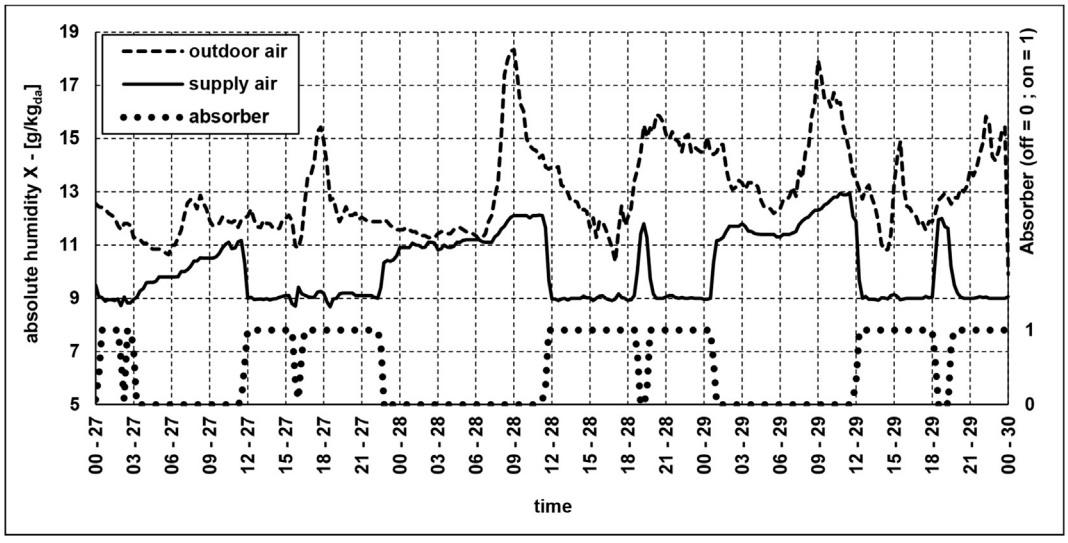


**Fig. A.1 – Trend of the outdoor air absolute humidity, supply air absolute humidity, absorber working status in a three days period (from July 27th 2011 to July 29th 2011 – air volume flow rate: 4500 $m^3\ h^{-1}$).**

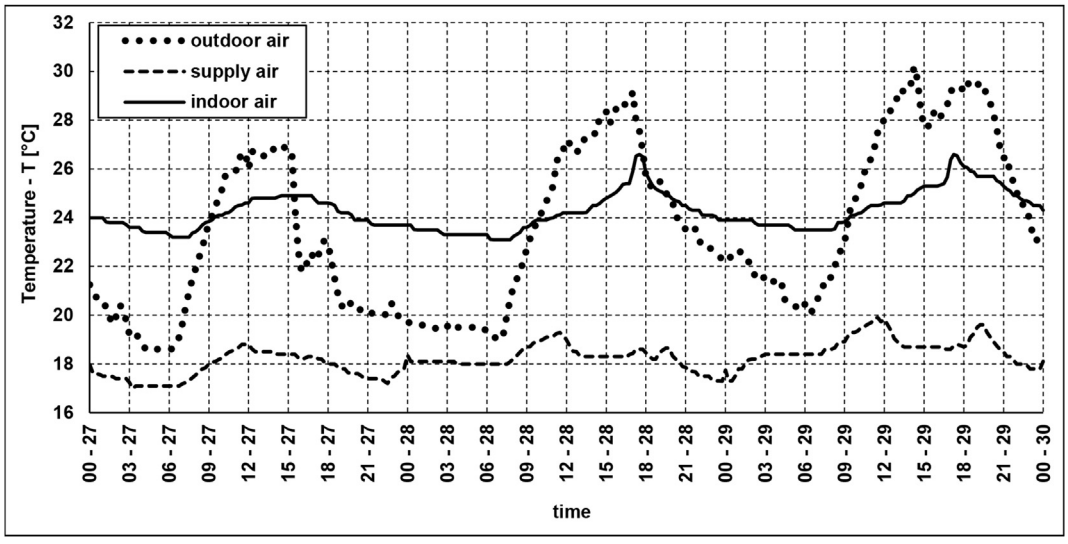


**Fig. A.2 – Trend of the outdoor air temperature, supply air temperature and indoor air temperature in a three days period (from July 27th 2011 to July 29th 2011 – air volume flow rate: 4500 $m^3\ h^{-1}$).**

Fig. A.2 shows that the outdoor air temperature varies in the range 18 °C ÷ 30 °C while the temperatures of the indoor air and the supply air at the entrance of the warehouse are constant, the former is at the set point value 24 °C ± 2 °C and the

latter is at 18 °C ± 1 °C. As the volume flow rate and the temperature of the supply air are constant, while the thermal loads and the outdoor air temperature are not, it follows that the cold water flowing in the fan coils removes part of the thermal load connected with the working activity and the weather conditions. It can be concluded that the desiccant evaporative cooler and the water network, working together, are able to keep the indoor air temperature at the set point and they can handle the variations of both the thermal loads and the weather conditions.

## Appendix B

The effect of weather conditions is described by means of three quantities, namely the outdoor temperature, the outdoor absolute humidity and the energy provided by solar irradiation. Since all of them vary in time, the statistical distribution during the plant operating period is useful to identify typical values. The procedure adopted for all the quantities is summarized in the following steps:

1. the maximum and the minimum values are sought to define the variation range of a quantity;
2. the variation range is divided in ten contiguous, non-overlapping, parts of equal span (rounded…) defining classes of data;
3. the number of samples falling in every class is counted in order to calculate the percentage of samples in that class; the information is reported in suitable charts, mainly histograms, for easier understanding;
4. the mean value and the standard deviation of the distribution are computed.

The statistical distribution of the outdoor air temperature (Figure B.1) ranges between 14 °C and 41 °C with 5 °C standard deviation, corresponding to 20% of the variation range. The histogram shows that the outdoor temperature varied significantly during the plant monitoring period and the width of the interval gathering 50% of the data, centered around the mean value (28.5 °C), is approximately two times the standard deviation (10 °C which corresponds, i.e. 40% of the span range).

The statistical distribution of the outdoor air absolute humidity (Figure B.2) is quite similar. The standard deviation is 2.5 g $kg_{da}^{-1}$, corresponding to 16% of the variation range (6 g $kg_{da}^{-1}$ ÷ 22 g $kg_{da}^{-1}$). The width of the interval gathering 50% of the data, centered on the mean value (12.7 g $kg_{da}^{-1}$), is approximately 25% of the variation range.

These results indicate that there are not typical values (meaning classes with number of samples significantly larger than the others) suitable for a daily-based analysis of the plant neither for the outdoor air temperature nor for the absolute humidity. On the other hand, the set points for supply air temperature and absolute humidity are constant, thus the plant operating conditions happen to change day by day. Hence, average quantities over the whole period appear the most suitable option to evaluate energy consumption.

Maximum, minimum and mean value of the solar irradiation during the plant operating period are represented in Figure B.3 while statistical distribution is reported in Figure B.4. The significant time variation as well as the non-uniform statistical distribution are a consequence of the combined effect of Earth motion and clouds.

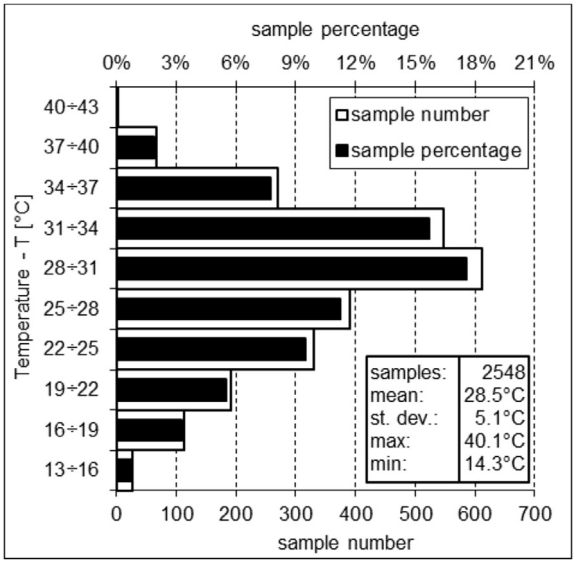


**Fig. B.1 – Temperature distribution during the operating period of the air conditioning system (07:00 ÷ 19:00).**

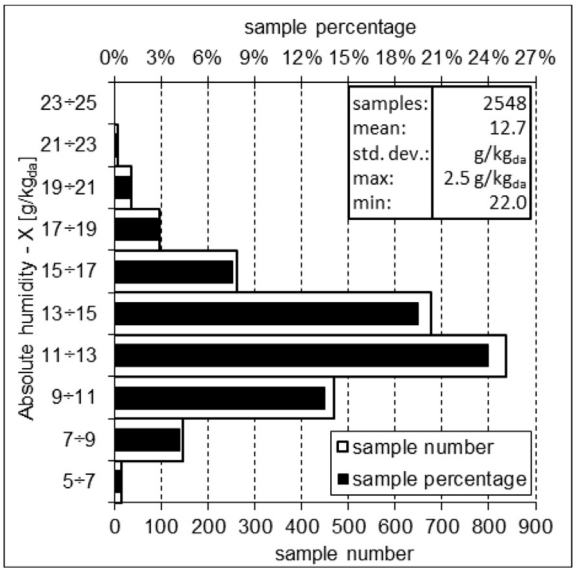


**Fig. B.2 – Absolute humidity distribution during the operating period of the air conditioning system (07:00 ÷ 19:00).**

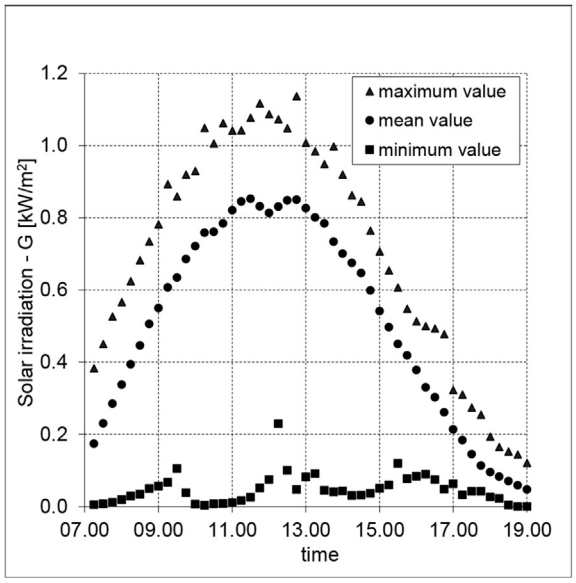


**Fig. B.3 – Maximum, minimum and mean value of solar irradiation during the operating period of the air conditioning system (07:00 ÷ 19:00).**

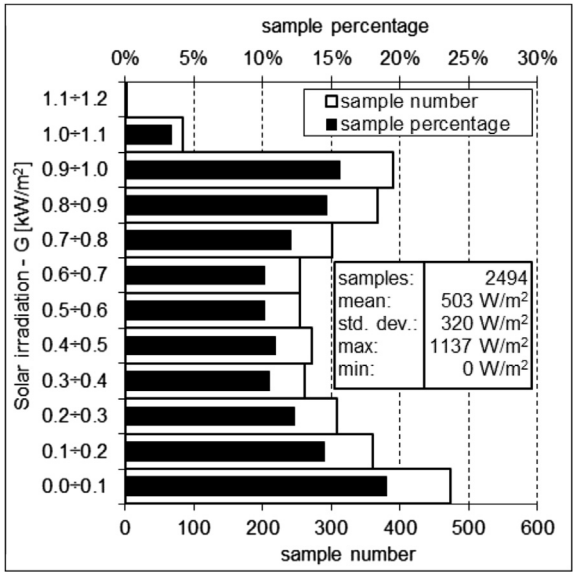


**Fig. B.4 – Solar irradiation distribution during the operating period of the air conditioning system (07:00 ÷ 19:00).**

Figs. B.5 and B.6 report the day-by-day variation of solar energy per square meter, referred to as specific solar energy, calculated by numerical integration of the solar irradiation data and its statistical distribution, respectively. The maximum value of the statistical distribution (29% of the samples in the range 23.5 ÷ 26.0 MJ $m^{-2}$) is considerably larger than the values observed for temperature or absolute humidity. However, the combined effect of the seasonal change (which is evident in Fig. B.5 as the decreasing trend of the daily specific solar energy due to the shortening of the days) and weather condition (random scatter of the data) induces the largest standard deviation (23% of the variation range). Hence, also in this case, the average value over the operating period appears the most suitable choice.

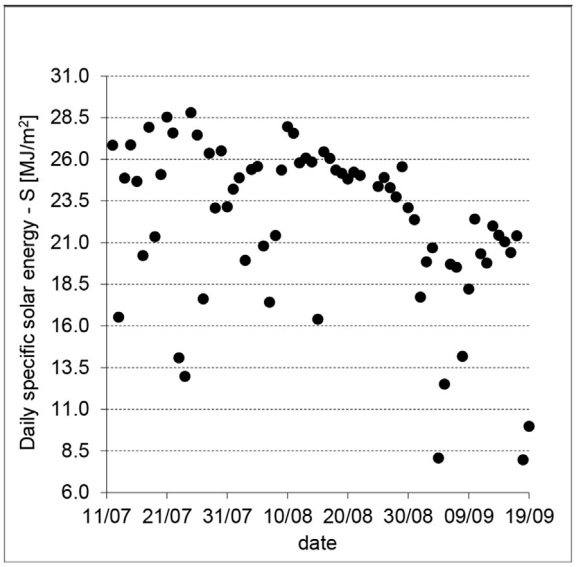


**Fig. B.5 – Daily solar energy received by a unit area surface during the operating period of the air conditioning system (07:00 ÷ 19:00).**

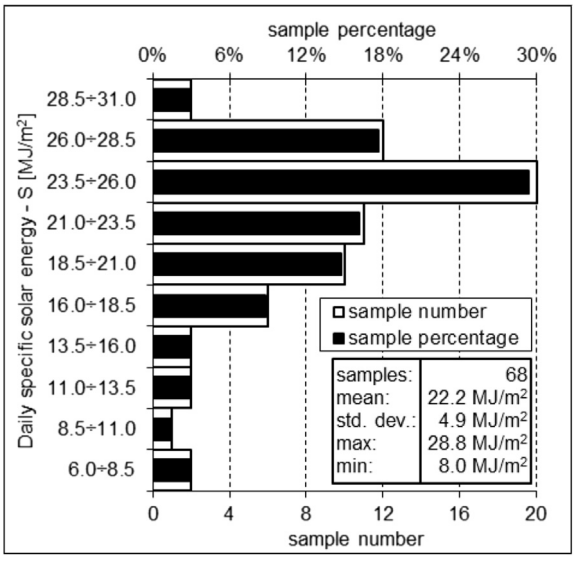


**Fig. B.6 – Distribution of the daily solar energy received by a unit area surface during the operating period of the air conditioning system (07:00 ÷ 19:00).**

## Appendix C

The sensitivity analysis to assess the dependence of the primary energy ratio (Equations (12) and (13)) and the primary energy saving index (Equation (14)) on the standard efficiencies is performed under the following assumptions:

1. boilers use natural gas, which is the most common fuel, thus the fuel combustion efficiency $\eta_f$ is kept constant;
2. the variation of the standard efficiencies is small.

Assumption 2 allows approximating the variation of any quantity due to the variation of the independent quantities as:

$$\Delta y = y(z_1 + \Delta z_1, z_2 + \Delta z_2, \ldots, z_n + \Delta z_n) - y(z_1, z_2, \ldots, z_n) = \sum_{j=1}^{n} \frac{\partial y}{\partial z_j} \Delta z_j \quad (C.1)$$

For sake of simplicity, the sensitivity analysis is performed in terms of percentage variation of the actual value.

$$\delta y = \frac{\Delta y}{y(z_1, z_2, \ldots, z_n)} \quad (C.2)$$

Consequently, percentage variations result:

$$\delta P_d = \frac{\delta\eta_e + \frac{Q_b \eta_e}{E_d \eta_f \eta_b} \delta\eta_b}{1 + \frac{Q_b \eta_e}{E_d \eta_f \eta_b}} \quad (C.3)$$

for the primary energy ratio of the desiccant evaporative cooler,

$$\delta P_e = \frac{\delta\eta_e + \frac{Q_b \eta_e}{E_e \eta_f \eta_b} \delta\eta_b}{1 + \frac{Q_b \eta_e}{E_e \eta_f \eta_b}} \quad (C.4)$$

for the primary energy ratio of the whole plant,

$$\delta F = \left(1 - \frac{1}{F}\right) \frac{\frac{1}{\eta_e \eta_b \eta_f} \left[ Q_b \left( \frac{Q_{c,0}}{COP_0} + E_0 \right) + Q_{b,0} E_e \right] (\delta\eta_b - \delta\eta_e) + \left( \frac{Q_b}{\eta_b \eta_f} + \frac{E_e}{\eta_e} \right) \frac{Q_{c,0}}{COP_0 \eta_e} \delta COP_0}{\left( \frac{Q_b}{\eta_b \eta_f} + \frac{E_e}{\eta_e} \right) \left( \frac{Q_{b,0}}{\eta_b \eta_f} + \frac{Q_{c,0}}{COP_0 \eta_e} + \frac{E_0}{\eta_e} \right)} \quad (C.5)$$

for the primary energy saving.

## REFERENCES


Alizadeh, S., 2008. Performance of a solar liquid desiccant air conditioner –An experimental and theoretical approach. Sol. Energy 82, 563–572.

Beccali, M., Finocchiaro, P., Nocke, B., 2009. Solar desiccant cooling system operating in Palermo (Italy): results and validation of simulation models. In: Proceedings of the OTTI Conference Solar Air Conditioning, Palermo.

Beccali, M., Finocchiaro, P., Nocke, B., 2012. Energy performance evaluation of a demo solar desiccant cooling system with heat recovery for the regeneration of the adsorption material. Renew. Energy 44, 40–52.

Crofoot, L., Harrison, S., 2012. Performance evaluation of a liquid desiccant solar air conditioning system. Energy Procedia 30, 542–550.

Daou, K., Wang, R., Xia, Z., 2006. Desiccant cooling air conditioning: a review. Renew. Sustain. Energy Rev. 10, 55–77.

Eicker, U., Schneide, D., Schumacher, J., Ge, T., Dai, Y., 2010. Operational experiences with solar air collector driven desiccant cooling systems. Appl. Energy 87, 3735–3747.

EN 15603 Energy performance of buildings – Overall energy use and definition of energy ratings, approved by CEN on 24 November 2007.

Finocchiaro, P., Beccali, M., Nocke, B., 2012. Advanced solar assisted desiccant and evaporative cooling system equipped with wet heat exchangers. Sol. Energy 86, 608–618.

Fong, K.F., Chow, T.T., Lee, C.K., Lin, Z., Chan, L.S., 2010. Comparative study of different solar cooling systems for buildings in subtropical city. Sol. Energy 84, 227–244.

Gommed, K., Grossman, G., 2007. Experimental investigation of a liquid desiccant system for solar cooling and dehumidification. Sol. Energy 81, 131–138.

Henning, H.M., 2004. Solar-assisted Air-conditioning in Buildings - Handbook for Planners. Springer, Wien, New York.

Henning, H.M., 2007. Solar assisted air conditioning of buildings - an overview. Appl. Therm. Eng. 27, 1734–1749.

IEA Task 38 Reports D-A3b Monitoring Results By Dagmar Jaehnig and Alexander Thuer.

Katejanekarn, T., Chirarattananon, S., Kumar, S., 2009. An experimental study of a solar-regenerated liquid desiccant ventilation pre-conditioning system. Sol. Energy 83, 920–933.

Kima, D.S., Ferreira, C.A., 2007. Solar refrigeration options – a state-of-the-art review. Int. J. Refrigeration 31, 3–15.

A. Napolitano, N. Sparber, A. Thür, P.Finocchiaro, B. Nocke, Monitoring Procedure for Solar Cooling Systems, A joint technical report of subtask A and B (D-A3a/D-B3b) Task 38 Solar Air-Conditioning and Refrigeration.

Rossetti, A., Viani, S., March 8, 2013a. Valutazione delle prestazioni di sistemi di solar cooling esistenti (Evaluation of the Performance of Existing Solar Cooling Plants). RdS 2010. www.rse-web.it.

Rossetti, A., Viani, S., March 8, 2013b. Analisi economica ed energetica di sistemi di solar cooling (Energetic ad Economical Analysis of Solar Cooling Systems). RdS 2011. www.rse-web.it.

Viani, S., Picenni, S., March 8, 2013. Stato dell'arte delle tecnologie per il solar cooling (State of art of solar cooling technologies. RdS 2009. www.rse-web.it.

Wiemken, E., April, 2009. Requirements on the Design and Configuration of Small and Medium Sized Solar Air-condition Applications. SOLAIR project. www.solair-project.eu. Zeidan, B., Aly, A., Hamed, A., 2011. Modeling and simulation of solar-powered liquid desiccant regenerator for open absorption cooling cycle. Sol. energy 85, 2977–2986.